7 July 1978, Volume 201, Number 4350

SCIENCE

An Unusual Lightning Flash at Kennedy Space Center

Cooperative research led to a comprehensive picture of the physics and meteorology of an unusual lightning flash.

Martin A. Uman, William H. Beasley, James A. Tiller, Yung-Tao Lin, E. Philip Krider, Charles D. Weidmann, Paul R. Krehbiel, Marx Brook, Arthur A. Few, Jr., Jerry L. Bohannon, Carl L. Lennon, Horst A. Poehler, William Jafferis, Jesse R. Gulick, James R. Nicholson

Summary. A lightning flash that struck the 150-meter weather tower at Kennedy Space Center was studied by several research groups using various techniques. The flash had unusually large peak currents and a stepped leader of relatively short duration. The charged regions neutralized by the three return strokes were located within a horizontal layer between heights of about 6 and 8 kilometers, where environmental temperatures were about $-10°$ to $-20°C$. The charge source for the first return stroke coincided with a vertical shaft of precipitation inferred to have been graupel or hail. Charge sources for subsequent strokes were near the edge of the detectable precipitation echo. The overall channel length was about 10 kilometers. A vertically oriented intracloud discharge occurred after the three return strokes.

During the summer of 1976, about 20 groups of experimentalists from universities and government laboratories joined at the National Aeronautics and Space Administration Kennedy Space Center (KSC), Florida, to initiate Thunderstorm Research International Program–1976 (TRIP-76) (*1*). The authors of this article represent six groups whose principal interests include lightning channel geometries inside and outside clouds, lightning currents and the variations of these currents with space and time, the locations and magnitudes of cloud charges that are neutralized by lightning, and the relationship of all of these to the structure of cloud precipitation patterns and wind fields.

On 19 July 1976, at about 16:20 universal time (U.T.), a typical afternoon thunderstorm formed over KSC. The storm lasted more than 90 minutes, producing about 140 intracloud and cloud-to-ground lightning discharges. The coverage of precipitation echoes at 17:00 U.T. detected by the KSC WSR-72X radar is shown shaded in Fig. 1.

At 16:59:59 U.T. a three-stroke lightning flash (*2*) struck the KSC 150-meter weather tower (see Fig. 1). In this article we present a detailed analysis of this lightning flash, including the locations and magnitudes of cloud charges neutralized by the discharge, the lightning channel geometry and currents, the locations of sources of very high frequency (VHF) radio emissions associated with the flash, radar precipitation data, and the relationships of these quantities to each other. We chose this particular flash for detailed study both because it struck the tower and because it produced peak currents that were among the largest ever recorded. We believe that the analyses presented in this article illustrate that cooperation among separate research groups, using a variety of current research techniques, can lead to an improved understanding of lightning discharge processes and their relationships to thunderstorm structure and dynamics.

Observational and Analytical Methods

The measurements of interest in this work are summarized in Table 1, and the sites at which they were made are shown in Fig. 1. Thunderstorm electric fields and the changes in these fields produced by lightning were recorded by using the KSC 25-station electric field-mill network, a system designed to help assess hazards to space vehicles from electrified clouds and lightning present before and during launch. Each field sensor had a response time of about 0.1 second. The errors in field values are estimated to be less than 10 percent (*3, 4*).

Measurements of the structure of electrostatic field changes caused by lightning were made by the group from the New Mexico Institute of Mining and Technology (NMIMT) at nine locations covering an area of 11 by 20 kilometers. Seven of the locations are shown on the map in Fig. 1, the other two being just off the map. These measurements had a time resolution of about 1 millisecond and a relative accuracy from station to station of a few percent.

The location and magnitude of the total cloud charge neutralized by a cloud-to-ground lightning flash can be inferred from the changes in the electrostatic field recorded at the 25 field-mill sites. The lo-

M. A. Uman, W. H. Beasley, J. A. Tiller, and Y.-T. Lin are in the Electrical Engineering Department, University of Florida, Gainesville 32611; E. P. Krider and C. D. Weidmann at the Institute of Atmospheric Physics, University of Arizona, Tucson 85721; P. R. Krehbiel and M. Brook in the Physics Department, New Mexico Institute of Mining and Technology, Socorro 87801; A. A. Few and J. L. Bohannon in the Space Physics and Astronomy Department, Rice University, Houston, Texas 77001; C. L. Lennon, H. A. Poehler, and W. Jafferis at the Kennedy Space Center, Florida 32899; and J. R. Gulick and J. R. Nicholson at the National Weather Service, Kennedy Space Center, Florida 32899.

0036-8075/78/0707-0009$02.00/0

cation and magnitude of the charge neutralized by each stroke in a flash can be determined from the NMIMT measurements of field change. The total charge is the sum of the stroke charges. In both cases, it is assumed that the original distribution of charge in a cloud is spherically symmetrical, a good approximation if the dimensions of the actual charge volumes are small compared to their height above ground. Making this assumption, the change E_{ci} in the field at a horizontal distance D_i from a charge Q a distance H above an infinitely conducting ground plane can be described by the relation

$$E_{ci} = \frac{1}{4\pi\epsilon_0} \frac{2QH}{(H^2 + D_i^2)^{3/2}} \qquad (1)$$

where the subscript i labels each recording site, and ϵ_0 is the permittivity of free space. With this relation, a computer search can be performed to find the Q, H, and D_i that minimize the function

$$x^2 = \sum_{i=1}^{N} \frac{(E_{mi} - E_{ci})^2}{\sigma_i^2} \qquad (2)$$

where E_{mi} is the measured field change at site i and σ_i is the root-mean-square measurement uncertainty (*3, 5*).

The rapid changes in electric and magnetic fields produced by return strokes were recorded at three stations by the groups from the universities of Florida and Arizona, using broadband antenna systems with overall 3-decibel bandwidths from about 0.2 hertz to about 1.5 megahertz, yielding a time resolution of about 0.2 microsecond (*6*). Two of the stations were located about 10 km apart at KSC, the third at Gainesville, Florida, about 200 km northwest. The locations of ground points struck by cloud-to-ground lightning at KSC were determined by using recently developed magnetic direction-finding techniques (*7*). Lightning-stroke currents were derived from the electric and magnetic fields measured at the three stations as discussed below (*8, 9*).

The waveform of the electric or magnetic field from the first return stroke of the flash that hit the 150-m tower admits of three interpretations: (i) the peak current in the tower was caused entirely by an upward-going streamer; (ii) the peak current was caused entirely by an upward-propagating return-stroke pulse; or (iii) the peak current was the result of a combination of both an upward-going streamer and a return-stroke pulse.

If the current in an upward-propagating streamer is approximately uniform with height, which is reasonable for short discharges, the peak current I_p can be found from the magnetic field change B, using

$$I_p = \frac{2\pi c D}{\mu_0 L(t_p)} \int_0^{t_p} \exp\left[-\frac{c}{D}(t_p - \tau)\right] \times B\left(\tau + \frac{D}{c}\right) d\tau \qquad (3)$$

where D is the stroke distance, $L(t_p)$ the streamer length at t_p, t_p the time yielding peak current, c the speed of light, and μ_0 the permeability of free space (*8*). On the other hand, if the magnetic field peak is caused by a return-stroke current pulse alone, then the relation needed is

$$I_p = \frac{2\pi c D}{\mu_0 V} \int_0^{t_p} \exp\left[-\frac{c}{D}(t_p - \tau)\right] \times \frac{dB}{d\tau}\left(\tau + \frac{D}{c}\right) d\tau \qquad (4)$$

where V, the return-stroke velocity, is assumed constant until the peak occurs (*8*).

For subsequent strokes, we use Eq. 4 and the magnetic field waveforms of the subsequent strokes to compute the peak currents. Current wave shapes of the subsequent strokes are determined by using the model and techniques developed from analyses of many multiple-station electric and magnetic field waveforms (*10*).

The 150-m tower was directly instrumented to estimate the peak lightning current. A long strip of magnetic tape on which an 8-kHz sine wave had been recorded was placed perpendicular to one guy wire of the tower to measure

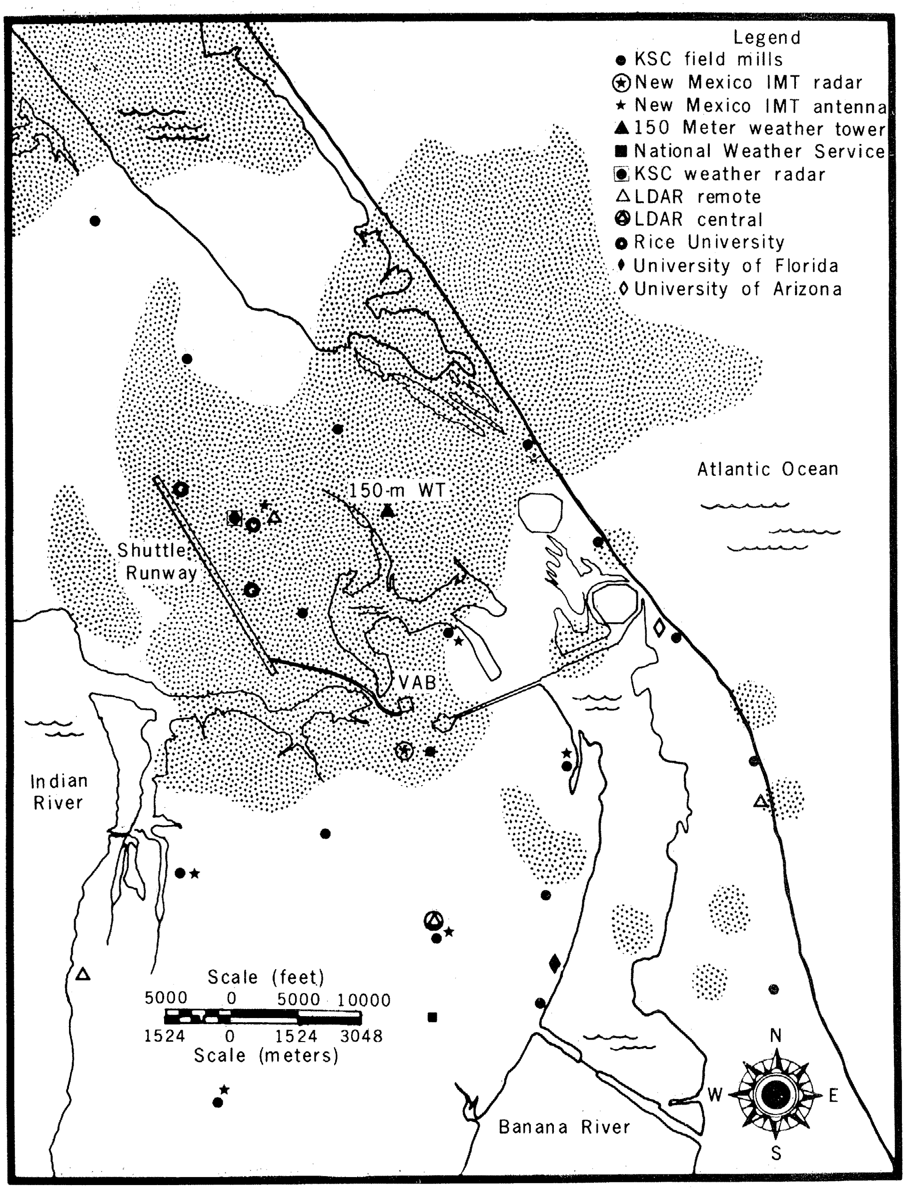

Fig. 1. Plan view of Kennedy Space Center (KSC) showing locations of measurement sites, the 150-m weather tower (*WT*), reference landmarks, and the radar precipitation echo (shaded area) at 17:00 U.T. obtained with a 2.9° elevation angle. Other abbreviations: *IMT*, Institute of Mining and Technology; *LDAR*, Lightning Detection and Ranging System; and *VAB*, Vehicle Assembly Building.

the peak current in the wire. The magnetic field of the current erases the signal on the tape out to a radius indicative of the peak current in the wire. Once the division of current among the tower and guy wires is determined from small-scale model experiments (*11*), the peak lightning current can be estimated. In addition to the strip of magnetized tape, a Rogowski coil was placed on the guy wire and was attached to a flashbulb set to fire when the rate of change of current in the guy wire exceeded 600 amperes per microsecond.

To locate lightning channels inside thunderstorms, the Rice University group operated three stations, each having four microphones and an electric field–change antenna (*12*). The microphones, with 3-dB bandwidths from about 0.1 to 450 Hz, were in a square array with 40- to 50-m sides oriented north-south and east-west at each station. The arrays, at the locations shown in Fig. 1, formed a triangle with sides of 1661, 1063, and 2445 m. The locations of the channel segments that produce thunder pulses are computed by solving for the unique point in space at which the range to each array corresponds to the measured time delay between the flash and the arrival of a corresponding thunder pulse at the array. For the data presented in this article we did not compensate for the effects of wind, wind shear, or temperature gradients on acoustic wave propagation. These effects are not large (*13*). The most significant source of uncertainty in determining the location of a channel segment is the thunder pulse duration (*14, 15*).

The KSC Lightning Detection and Ranging System (LDAR) (*16*) detects electromagnetic pulses in the band 30 to 50 MHz radiated by electric discharges in thunderstorms. The locations of these discharges are determined by measuring the differences between the times of arrival of the pulses at five stations arranged in several four-station Y configurations. Remote stations use logarithmic intermediate-frequency amplifiers as receivers, employing successive detection to detect the envelopes of the radio-frequency pulses. The resulting signals are transmitted to a central station over wideband (5 MHz) communication circuits. At the central station the signal waveforms are digitized every 0.05 μsec for 100 μsec. Signals are analyzed in digital form by computer to find the source locations from the differences in time between the peak signals at the individual stations and the central station. Data samples of this type can be taken at rates up to 400 per second. The actual rate at which radiation source locations are fixed, typically 100 per second, is a function of the trigger level selected and the activity of the discharges. Errors in source locations are minimized by using the Y configuration of stations. Experimental errors are estimated by comparing the results from two different Y configurations. For about half the locations discussed in this article the errors

Table 1. Groups participating in the study and measurements from which data presented in this article were derived. The number of stations for each group is also given.

Group	Measurement	Number of stations
NASA Kennedy Space Center	Location of sources of 30- to 50-MHz radiation (LDAR)	5*
	Field mills (measurements)	25†
National Weather Service	KSC radar	1
	KSC radar display, visual observations	1
New Mexico Institute of Mining and Technology	Fast scanning radar	1
	Electric field-change antennas	9‡
Rice University	Thunder	3
University of Arizona	KSC field mills (analysis)	25
	Broadband electric and magnetic field changes	1
University of Florida	Broadband electric and magnetic field changes	2§

*One not shown in Fig. 1. †Seven not shown in Fig. 1. ‡Two not shown in Fig. 1. §One (in Gainesville) not shown in Fig. 1.

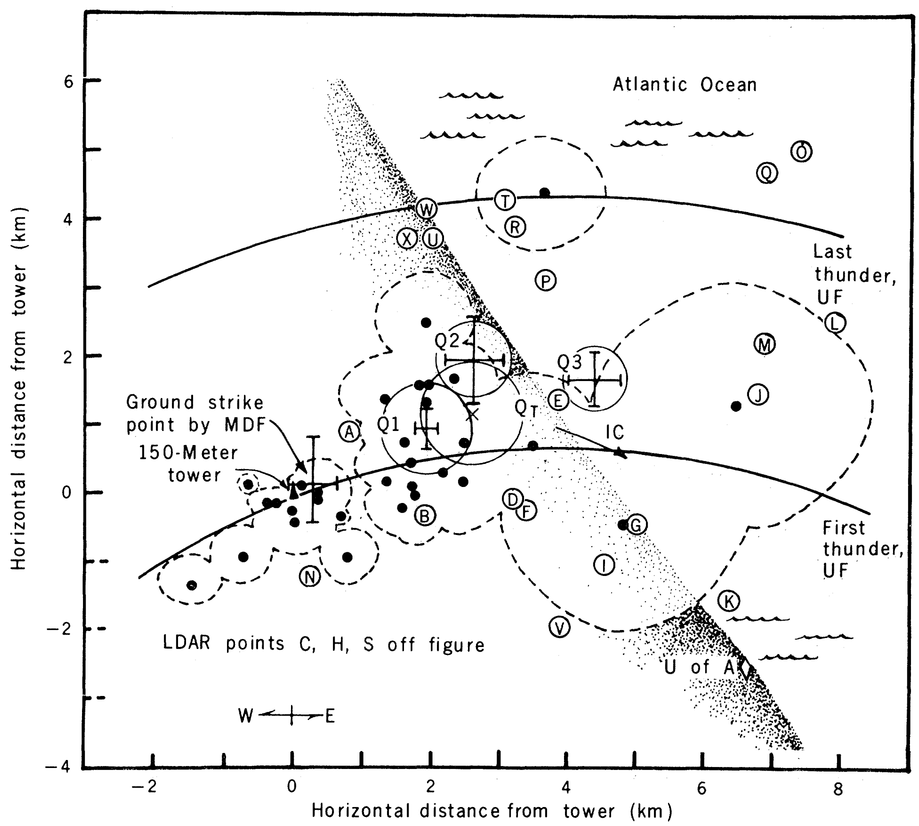

Fig. 2. Plan view of Kennedy Space Center showing data for the lightning flash at 16:59:59 U.T. Solid dots represent sources of thunder from points along the lightning channel. Dashed curved lines mark the envelope of maximum uncertainty in thunder source locations. The ground strike point determined by magnetic direction finding (*MDF*) is shown near the tower, with error bars. Solid arcs show the distances corresponding to the first and last thunder recorded at the University of Florida (*UF*) station, assuming the thunder traveled at a speed of 350 m/sec, from sources near ground. The circle labeled Q_T shows the location of the -39 C charge computed for the whole flash including the intracloud portion, with the circle showing the size of an equivalent spherical charge distribution of density -20 C/km^3. The centers of the circles labeled Q_1, Q_2, and Q_3 mark the locations of the charges -25, -14, and -8 C, respectively, lowered by the three return strokes; the error bars show the uncertainty in location and the circles represent the size of an equivalent spherical charge distribution of density -20 C/km^3. The arrow labeled *IC* shows the approximate location and orientation of a dipole charge which, when neutralized, would give the measured moment change of the first 17 msec of the intracloud portion of the discharge. The small circles circumscribing letters *A* through *X* mark the locations of sources of 30- to 50-MHz radiation in order of occurrence at the times shown in Fig. 5.

in all three dimensions were about 100 to 200 m; for the remaining points they ranged up to several kilometers.

Two microwave radar systems were used to examine the precipitation structure of storms at KSC. Both were incoherent pulsed systems operating at a wavelength of about 3 centimeters. One, the WSR-72X, provided selected constant-elevation or constant-azimuth scans at about 20-second intervals. The other, a fast-scanning system (*17*), was operated by NMIMT at the location shown in Fig. 1 near the center of the field-mill and NMIMT antenna networks. Its antenna scanned in elevation at a rate of 3 revolutions per second and rotated one beam width in azimuth (3°) during each elevation scan, providing full coverage of the hemisphere overhead every 20 seconds. To be able to scan rapidly and still obtain a good estimate of reflectivity, the radar transmits pulses of broadband noise of bandwidth BW = 30 MHz, with a short coherency time $t = 1/\mathrm{BW} \simeq 0.03$ μsec compared to the time intervals of the desired resolution in range (1 μsec or 150 m). With such a transmitted signal, the normally large pulse-to-pulse fluctuations caused by interference between the constantly rearranging scatterers is reduced by averaging the return in range for a time corresponding to the desired range resolution. For the fast-scanning system, transmitted power was 20 kilowatts in a pulse length of 0.3 μsec at a pulse repetition frequency of 3 kHz.

Lightning in the Storm of 19 July 1976

The field-mill records show that there were about 130 field changes caused by cloud-to-ground and intracloud lightning flashes between about 16:24 and 17:52 U.T. (*4*). The NMIMT network of nine antennas recorded about 137 flashes between 16:21 and 17:52 U.T., including 31 ground flashes over KSC during the time between 16:41 and 17:48. During the period from about 16:49 to about 17:20 U.T., 55 electric field changes of 125 volts per meter or more (for an entire flash) were recorded at the University of Florida station, indicating that number of flashes in the KSC area. Of these, 17 were cloud-to-ground flashes with sufficient electrostatic field values after 170 μsec to indicate that they were within about 15 km (*18*, *19*). The ground contact points of 15 of the 17 flashes were located to within about 1 km by means of magnetic direction finding and thunder ranging from the stations operated by the University of Florida and the University of Arizona.

At about 16:59:59 U.T. an observer in the National Weather Service office at KSC headquarters saw a flash strike the 150-m weather tower. An observer at the University of Arizona station also saw a flash in the direction of the weather tower at that time. The magnetic tape attached to a guy wire indicated that the tower had been struck. In addition, the flashbulb connected to the Rogowski coil and mounted on the same guy wire had fired. No other flashes were observed to strike the tower, either visually or by magnetic direction finding. The various records of electric field change show that the flash occurred at 16:59:59 U.T. and had three return strokes followed by an intracloud discharge.

Figures 2 and 3 show plan and elevation views of the KSC area together with data indicating the geometry of the flash, the charge locations and magnitudes, and other pertinent features of the flash. The location of and uncertainty in the nominal ground contact point, as determined by magnetic direction finding from the University of Florida and University of Arizona stations, are shown by the error bars next to the tower symbol. The calculated strike point is within about 300 m of the tower, with a maximum uncertainty of about 750 m.

The two large solid arcs labeled "First Thunder, UF" and "Last Thunder, UF" in Fig. 2 mark the intersections with ground of two hypothetical concentric spherical surfaces centered on the University of Florida station. The radii of the surfaces are the distances obtained by multiplying the times to first thunder and last thunder by an assumed sound speed of 350 m/sec (305°K). The first surface intersects the ground 100 m or less from the tower. The first thunder to arrive at the University of Florida station could have originated from anywhere on this surface. The higher in altitude the origin of a particular thunder pulse, the farther south it would appear in the plan view of Fig. 2, in agreement with the results of the lightning channel reconstruction from thunder measurements by the group from Rice University; these results are shown in Figs. 2 and 3 as solid dots.

From the Rice data, the identifiable source of thunder closest to the tower was about 300 ± 900 m above and 300 ± 200 m south of the top of the tower. According to the calculations, the channel extended nearly vertically from

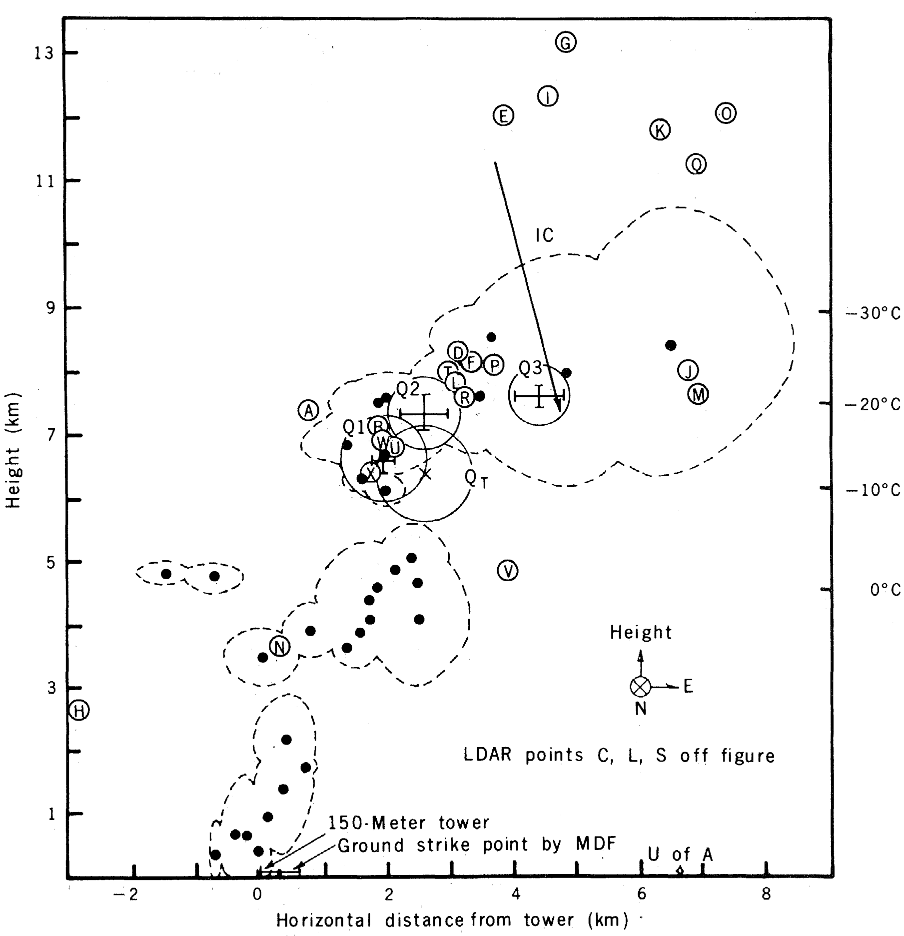

Fig. 3. Elevation view of the data presented in Fig. 2. Environmental air temperatures at 21:15 U.T. are shown on the right.

the tower to a height of 7.6 km (−20°C), where it turned abruptly horizontally and eastward for about 6.5 km from the tower. Not clearly shown in Figs. 2 and 3, but evident from detailed analyses, were a major branch reaching within about 370 m of the ground about 700 m west of the tower and extensive branching at altitudes of 5 and 7 km. The acoustic signal from the horizontal section of the channel was of low amplitude because that part of the channel was nearly parallel to the line of propagation to the microphone arrays, a situation that makes analysis difficult (*14*). To avoid confusion in Figs. 2 and 3, only the envelope of the uncertainties in channel location, shown as dashed lines, is given. Because the envelope is dominated by the points with the largest uncertainties, it represents the worst case with all data included.

The data points in Fig. 4 show the electric field changes produced by the entire flash as measured at 24 field mills (one field mill was not working at the time) of the KSC network. The field-change values are plotted as a function of horizontal distance from the computed location of the charge. The solid line represents the best fit to the data determined by minimizing Eq. 2. The charge computed for the whole flash was about −39 coulombs and was located at the position of the small cross inside the circle labeled Q_T in Figs. 2 and 3. This circle represents the spherical volume that would contain −39 C of charge if the charge density were a uniform −20 C/km^3, an

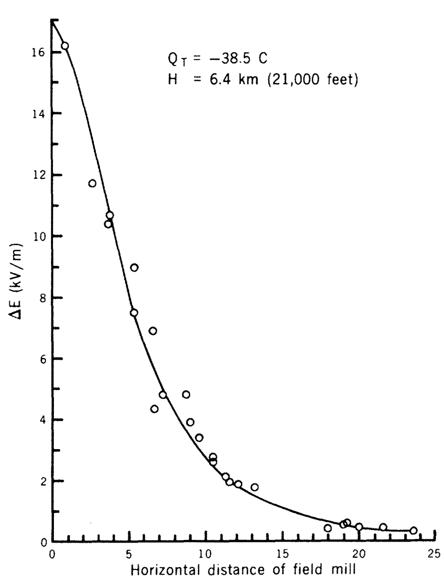

Fig. 4. Electric field change for the entire flash as a function of horizontal distance from the computed center of the charge producing the flash at 16:59:59 U.T. The points represent measurements at 24 field mills. The solid line is the calculated field change for the optimum values of Q, H, and D_i that satisfy Eq. 2.

arbitrary but plausible value for indicating the approximate extent of the charged region.

The antenna systems operated by NMIMT, the University of Florida, and the University of Arizona had sufficient time resolution to delineate the electric field changes for each return stroke of the flash at 16:59:59 U.T., as shown in Fig. 5.

Centers of charge corresponding to the field changes of the individual return strokes are denoted by the circles labeled Q_1, Q_2, and Q_3 in Figs. 2 and 3. As before, the size of the circle represents the amount of charge. The error bars specify the estimated error in location. Computed values of the charge neutralized by each stroke were −25, −14, and −8 C, for a total of −47 C. The charge centers are displaced horizontally away from the main return-stroke channel to ground and slightly upward with increasing stroke order, between environmental temperature levels of about −10° and −20°C. These levels agree well with those of charges measured previously for lightning in Florida and other regions (*3*). The sum of the charges for individual strokes is slightly larger than the charge for the whole flash, Q_T, obtained from the field-mill data, and the centroid of their locations is several hundred meters higher than the location of Q_T. These differences occur partly because the field-mill data included field change caused by the intracloud discharge following the third return stroke. As shown in Fig. 5, the intracloud field change was positive at the near stations and negative at the far ones, consistent with neutralization of an electric dipole with an upper positive charge and a lower negative charge.

Analysis of the intracloud field change in terms of a dipole model suggests that it was predominantly vertical. A dipole moment change of 140 C-km occurred within a time interval of 235 msec. During the first 17 msec of the intracloud discharge, the best dipole fit to the data is denoted by the downward-pointing arrow in Figs. 2 and 3 and corresponds to a moment change of 45 C-km. The length of the arrow indicates the distance over which an assumed 10 C of charge would have been neutralized; with this reasonable value assumed for the charge, the lower end of the inferred dipole lies at about the same altitude as the return-stroke charges and is adjacent to the charge source for the third stroke.

Average leader velocities can be estimated by using approximate leader durations determined from the electrostatic field records and approximate leader lengths determined from cloud charge locations and channel geometry. We assume that each leader traveled from its charge source along the path indicated by the thunder data as shown in Figs. 2 and 3. The first-stroke leader field change is indicative of a normal leader lowering negative charge, except that its duration, about 4 msec, is shorter than that of normal first leaders (*20*). On the other hand, there were several other first return-stroke leaders with short duration during the storm at KSC on 19 July 1976. The first leader, approximately 8 km long, had an average velocity of about 2×10^6 m/sec, an order of magnitude faster than the typical values but in the upper range of values obtained in South Africa (*20*), the best available source of statistical data on leader velocities. The second leader, about 9 km long, lasted either 3.4 msec or 280 μsec, depending on which portion of the field change one associates with the leader, yielding an average velocity of 2.7×10^6 or 3.3×10^7 m/sec. The third leader had a duration of 2.8 msec, a length of about 11 km, and a velocity of about 4×10^6 m/sec. Dart

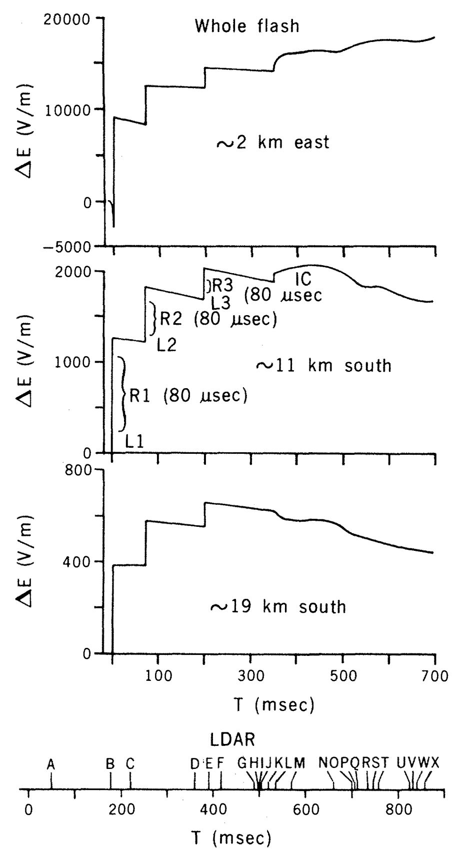

Fig. 5. Electric field changes at 16:59:59 U.T. 2, 11, and 19 km from the flash. Time of occurrence of *LDAR* fixes is given at the bottom. On the 11-km field, the leader portions of the field changes are labeled *L1*, *L2*, and *L3*, and extend from the bottom of the *R* bracket downward to the field break; the return strokes are bracketed and labeled *R1*, *R2*, and *R3*; the intracloud discharge beginning around 360 msec is labeled *IC*.

leaders have typical velocities in South Africa of 2×10^6 m/sec with upper limits an order of magnitude greater (*20*).

The small circles with letters inside in Figs. 2 and 3 represent locations of sources of VHF radiation determined by the LDAR system. The letters are in order of occurrence, at the times shown along the line at the bottom of Fig. 5. Almost all the VHF radiation occurred after the return strokes were over, and some appeared to be associated with the intracloud discharge. A large group of LDAR data points occurred at heights between 6 and 8 km, which roughly correspond to the heights of charge centers Q_1, Q_2, and Q_3 of Fig. 3. A second group of discharges occurred between 11.5 and 13 km, perhaps indicating the top of the intracloud discharge. It is interesting to note the absence of discharges along the lower half of the lightning channel, indicating that radiation in the 30- to 50-MHz band is much weaker from the leader and return-stroke channel than from discharges in the cloud.

The locations of charged regions Q_1, Q_2, and Q_3 are compared with the fast-scanning radar measurements of the precipitation structure of the storm in Fig. 6, a and b. Figure 6 shows vertical cross sections of the logarithmic radar return obtained at two azimuth angles through the storm several seconds after the flash occurred. The radar was located at the center of the concentric 5-km range circles. Figure 6a was obtained at an azimuth angle of 16.7° (clockwise from north), and the radar cross section passed through the apparent sources of charge for the first two strokes to ground. The charge source for the first stroke was within a tall vertical shaft of precipitation, and that for the second stroke was just beyond the vertical shaft in a region of weaker echo. The second radar cross section (Fig. 6b) was obtained at an azimuth angle of 31.7° and passed through the estimated source charges for the third stroke to ground and the intracloud discharge. Both discharges occurred along the far edge of the detectable precipitation echo. There was no absolute calibration for the radar data because on the day they were taken the receiver sensitivity was intermittently low and changing, but it is known that only the stronger precipitation echoes were being detected.

Several features of the radar data are worth noting. In Fig. 6a there is a striking periodic structure of the precipitation echoes on a scale of about 1 km. The precipitation echoes in both radar cross sections show a marked discontinuity at about the 4-km level, being stronger below it and weaker above it. The discontinuity is below the level of the environmental (clear air) 0°C isotherm (at 4.6 km), which suggests that the discontinuity was associated with the melting (and consequent increase in reflectivity) of ice-form precipitation particles. The ice-form precipitation most likely would have been graupel or hail rather than snow (*21*). Snow crystals have a lower velocity of fall and produce characteristic "bright band" echoes, which are observed during decaying stages of storms (*22*). On the basis of these observations, we infer that the lightning charge resided, at least in part, within a region of graupel or hail, between the −10° and −20°C environmental temperature levels. Observations of a similar correlation between lightning charge and precipitation have been made recently in New Mexico (*5*).

Figure 7 shows the electric and magnetic fields of the three return strokes, measured with time resolution of about 0.2 μsec on the broadband system at the University of Florida station approximately 11 km from the flash. The electric field changes measured by the broadband antenna systems were unusually large, as shown in Fig. 8, where histograms of the initial electric radiation field peaks, normalized to 100 km, are plotted for 10 first strokes and 23 subsequent strokes at known distances during the

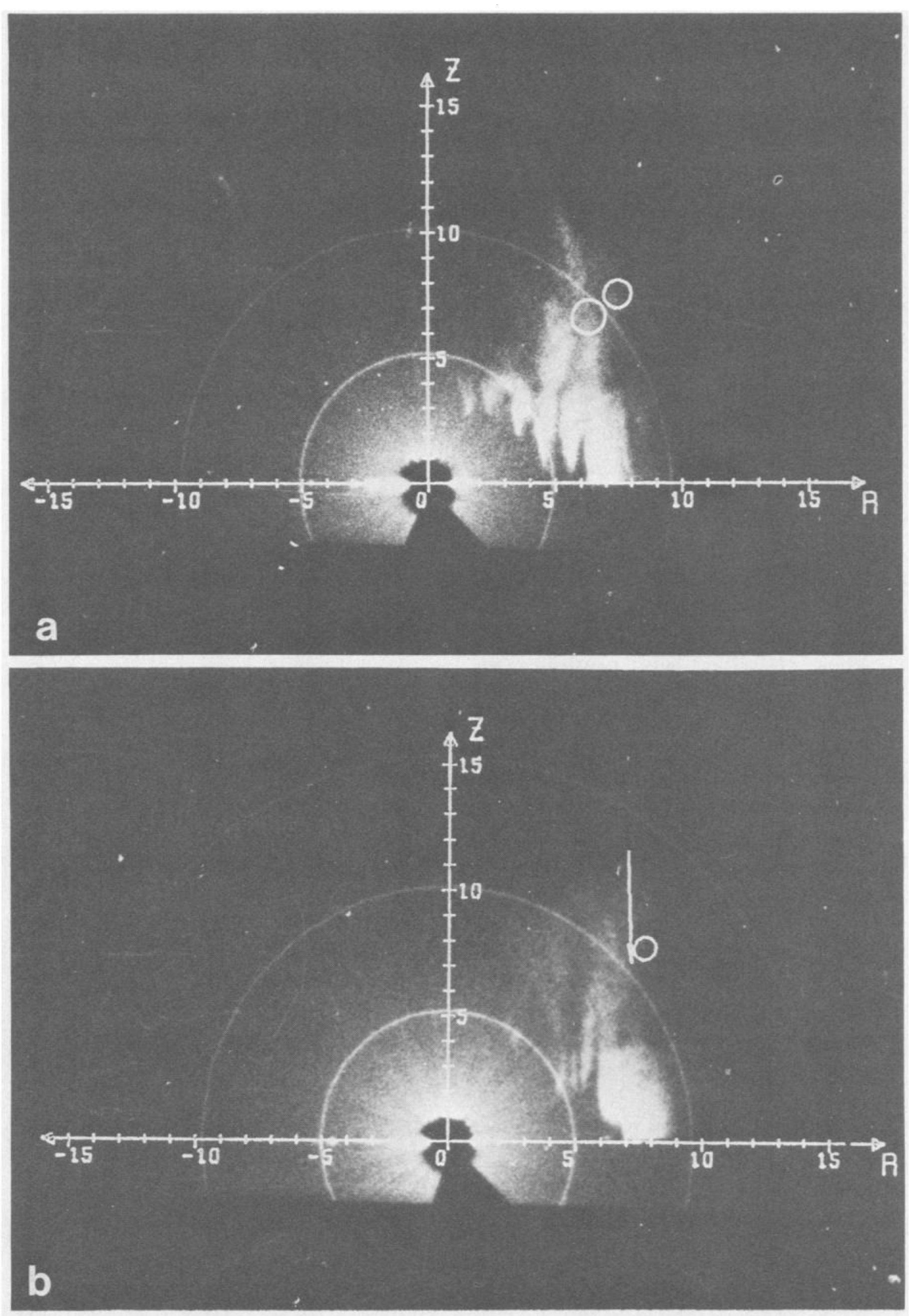

Fig. 6. Precipitation echoes obtained with high time resolution by fast-scanning radar, with charge locations superimposed. The radar cross sections were obtained at azimuth angles of (a) 16.7° and (b) 31.7°.

storm. The most frequent value of normalized field change was 2 to 3 V/m for subsequent strokes and the largest value was 8 to 9 V/m, except for the flash at 16:59:59 U.T. The second and third strokes of that flash had normalized peak radiation fields of about 39 and 13 V/m, respectively. Similarly, the normalized first-stroke radiation peak, 37 V/m, at 16:59:59 U.T. was about four times as large as the most frequent value, 8 to 9 V/m, for the others in the storm, not quite twice as large as the next largest. The most frequent values of peak radiation fields measured in the storm are consistent with the values measured previously in Florida, the largest of which was about 30 V/m. On the basis of the data in Fig. 8 and similar data obtained previously, we estimate that less than 1 percent of lightning occurrences have peak fields greater than 35 V/m (*18*). Similarly, the high peak currents associated with these fields should occur less than 1 percent of the time.

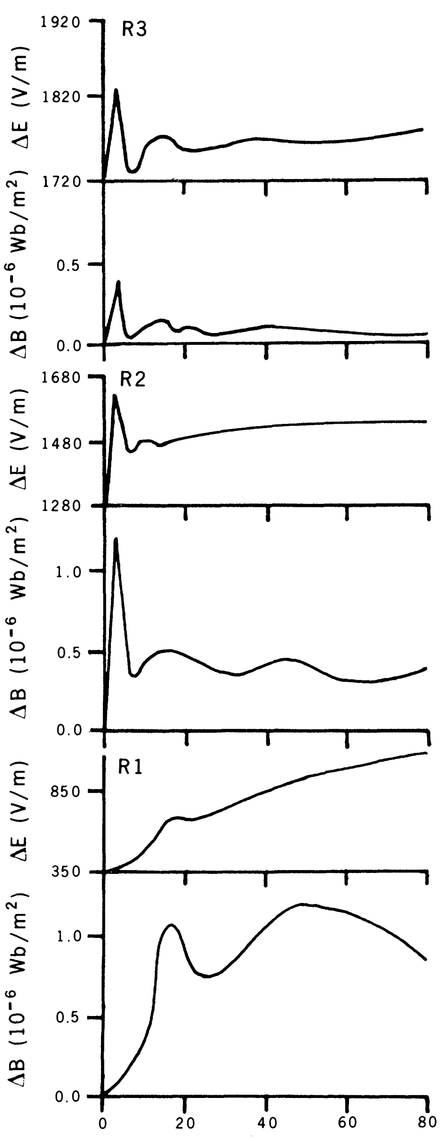

Fig. 7. Details of the three return-stroke electric field changes shown in Fig. 5, with the corresponding magnetic field changes, as observed 11 km from the flash. The return strokes are labeled *R1*, *R2*, and *R3*, as in Fig. 5.

The first stroke of the flash, as shown in Fig. 7, had an electric field rise time (zero to peak) of about 14 to 16 μsec, three to five times the usual value. This long rise time led us to consider the possibility that the first return stroke had an unusually long upward-going streamer. Rise times for subsequent strokes were 3.0 and 2.5 μsec, not unusual for Gainesville, but somewhat longer than typical rise times at KSC (*18, 23*). If we assume that the first-stroke magnetic field before peak in Fig. 7 was caused by an upward-going streamer extended about 300 m above the top of the 150-m tower (a velocity of about 2×10^7 m/sec for about 14 to 16 μsec), we calculate a peak current of approximately 210 kA from Eq. 3. In this case the peak current occurs at the ground at 24 μsec, about 10 μsec after the magnetic field peak.

To estimate the peak current under the assumption that it was caused by an upward-propagating return-stroke current pulse, we use Eq. 4. Since we had no measurement of the return-stroke velocity for this flash, we used values found in the literature. We analyzed the bottom portions of published photographs of eight first (highly branched) return strokes (*24, 25*) and found a return-stroke velocity of $8.8 \pm 3.4 \times 10^7$ m/sec (mean ± standard deviation). A later study of five first return strokes (*26*) yielded a mean velocity near ground of $5.9 \pm 3.1 \times 10^7$ m/sec. Using these results, we assume that the first return-stroke velocity may range from 2.8×10^7 to 1.2×10^8 m/sec, yielding a range of peak currents between 150 kA (1.2×10^8 m/sec) and 640 kA (2.8×10^7 m/sec). The peak current occurs in this case at the same time as the magnetic field peak. If the initial magnetic field was caused by both an upward-going leader and a return-stroke current pulse, a reasonable estimate of peak current at the ground would be 150 kA or more.

As noted earlier, the subsequent-stroke electric field waveforms shown in Fig. 7 allow channel currents to be modeled as upward-propagating current pulses. The mean velocity of 27 subsequent return strokes measured from published stroke photographs (*25*) is $4.7 \pm 2.4 \times 10^7$ m/sec. Two later studies yield mean subsequent return-stroke velocities of $8.0 \pm 2.0 \times 10^7$ m/sec (*26*) and $6.8 \pm 2.3 \times 10^7$ m/sec (*27*). Assuming that the range of subsequent-stroke velocities is 2.3×10^7 to 1.0×10^8 m/sec and using Eq. 4, we calculate that the peak current of the second stroke was between 200 and 870 kA and that of the third stroke was between 66 and 280 kA. The current wave shapes at the ground for the first 40 μsec of subsequent strokes, calculated by three-station techniques (*10*), are roughly the same as the corresponding magnetic field wave shapes at 11 km (see Fig. 7). Rise times of subsequent return-stroke currents are 2 to 3 μsec. The rise times of both first and subsequent return-stroke currents in the flash are consistent with those measured directly on towers struck by lightning. The shapes of the current waveforms derived for the subsequent strokes in this flash are similar to those measured directly on towers, except that the peaks in this case are sharper than those generally observed on towers (*28*).

The magnetic-tape measurements of peak current made by KSC personnel gave a value of about 14 kA in the guy wire and an estimated total peak lightning current of about 190 kA (*11*), in good agreement with the values determined from remote electric and magnetic field measurements.

Peak currents in the 200-kA range are equal to the largest values ever recorded by using magnetic links (*29*). Flashes with peak currents greater than 200 kA were at the 0.1 percent level in frequency of occurrence for 2721 flashes recorded throughout the United States. Peak currents above 200 kA are at about the 1 percent level, based on analyses of many measurements (*30*). Clearly, peak currents of 200 kA or more occur infrequently. It is interesting to speculate about whether the short duration of the stepped leader, the unusually large fields and peak currents, and the relatively slow first-stroke electric and magnetic fields and current rise times were caused by the presence of the 150-m tower.

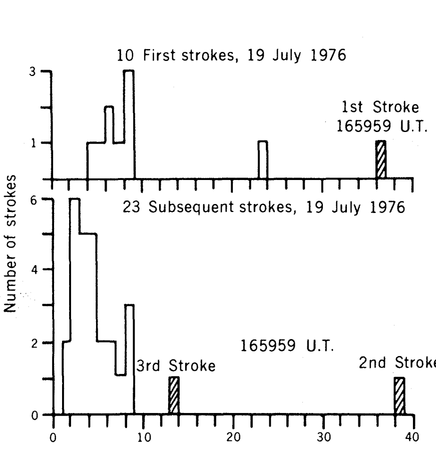

Fig. 8. Histograms of initial peak values of the electric radiation field for 10 first strokes and 23 subsequent strokes in 15 flashes during the storm at KSC on 19 July 1976.

Concluding Remarks

Lightning studies are difficult to carry out because of the unpredictable nature of thunderstorms and the variety and complexity of measurements necessary to derive significant information. It is perhaps remarkable that the various independent measurements obtained in this study led to results that are entirely consistent with one another. For example, the location of the ground strike point was accurately determined by both thunder and magnetic measurements. The locations of the charged regions determined from independent sets of data were in good agreement with each other and with the channel geometry determined from thunder measurements. Cooperative work such as that reported here can provide much more insight about lightning discharges and their relationships to the thunderstorm environment than could have been obtained with only independent observations. The results described here represent the most comprehensive study ever made of a single lightning flash and its relation to the thunderstorm which produced it.

References and Notes

1. E. T. Pierce, *Bull. Am. Meteorol. Soc.* **57**, 1214 (1976).
2. An entire discharge to ground lasts typically 0.5 second and is called a flash. The flash is composed of individual discharges called strokes; each stroke lasts for milliseconds and the time between strokes is tens of milliseconds. There are typically three or four strokes per flash, the minimum being one, the maximum measured 26. The first stroke in a cloud-to-ground flash is initiated by a stepped leader, which lowers negative charge from the cloud toward earth. When the stepped leader nears the ground, the electric field there is sufficient to cause streamers to be initiated and propagate upward to meet the leader tip. At the junction of the downward-moving leader and the upward-moving streamer the "return stroke" wave front forms and thereafter propagates upward, carrying ground potential into the cloud. The return stroke typically causes ground and channel currents of 10 kiloamperes rising to peak value in ~1 microsecond. Ordinarily, the upward-moving streamer goes a few tens of meters. In the case of tall buildings or towers, upward-moving streamers may become upward-going leaders extending a distance of one or two times the height of the tall object before being met by the downward-moving stepped leader. Sometimes the upward-going streamer extends all the way into the cloud. In this case, a return stroke does not occur. After the first stroke is completed and some tens of milliseconds have passed, a dart leader may lower negative charge down the previous return-stroke channel to the ground, initiating a subsequent return stroke. Dart leaders are not thought to induce appreciable upward streamers. For more details see (*9*).
3. E. T. Jacobson and E. P. Krider, *J. Atmos. Sci.* **33**, 103 (1976).
4. J. M. Livingston and E. P. Krider, *J. Geophys. Res.* **83**, 385 (1978).
5. P. R. Krehbiel, M. Brook, R. A. McCrory, D. Tarbox, in *Preprint Volume, International Conference on Cloud Physics* (American Meteorological Society, Boston, 1976), pp. 642–643; P. R. Krehbiel, M. Brook, R. A. McCrory, in preparation.
6. The broadband systems were similar in all important respects to those described by R. J. Fisher and M. A. Uman [*J. Geophys. Res.* **77**, 399 (1972)], E. P. Krider and R. C. Noggle [*J. Appl. Meteorol.* **14**, 252 (1975)], and E. P. Krider, C. D. Weidmann, and R. C. Noggle [*J. Geophys. Res.* **82**, 951 (1977)].
7. E. P. Krider, R. C. Noggle, M. A. Uman, *J. Appl. Meterol.* **15**, 301 (1976); B. D. Herrman, *et al.*, *ibid.*, p. 402.
8. M. A. Uman and D. K. McLain, *J. Geophys. Res.* **75**, 5143 (1970). Equation 3 here is equation 4 of Uman and McLain, and Eq. 4 here is equation 11 of Uman and McLain.
9. M. A. Uman, *Lightning* (McGraw-Hill, New York, 1969).
10. Y. T. Lin, M. A. Uman, E. P. Krider, *Eos* **57**, (Abstr.) 924 (1976).
11. S. Livermore, *NASA Tech. Rep. TR-1482* (1976).
12. A. A. Few, in *Preprint Volume, Conference on Cloud Physics* (American Meteorological Society, Boston, 1974), pp. 387–390; ——— and T. L. Teer, *J. Geophys. Res.* **79**, 5007 (1974); A. A. Few, *ibid.* **75**, 7517 (1970).
13. D. R. MacGorman, thesis, Rice University, Houston, Texas (1977).
14. A. A. Few, *Eos* **55**, 508 (1974).
15. ———, *Sci. Am.* **233**, 80 (July 1975).
16. C. L. Lennon, *Minutes of Frequency Management Group, Range Commander Council* (R1-R25, White Sands Missile Range, N.M., 1975).
17. M. Brook and P. R. Krehbiel, in *Preprint Volume, 16th Conference on Radar Meteorology* (American Meteorological Society, Boston, 1975), pp. 26–30.
18. J. A. Tiller, M. A. Uman, Y. T. Lin, R. D. Brantley, *J. Geophys. Res.* **81**, 4430 (1976).
19. M. A. Uman, J. A. Tiller, W. H. Beasley, E. P. Krider, C. D. Weidmann, *Eos* **57**, (Abstr.) 924 (1976).
20. B. F. J. Schonland, in *Handbuch der Physik*, S. Flugger, Ed. (Springer-Verlag, New York, 1956), pp. 576–528.
21. During TRIP 76-77, penetration of similar clouds by an instrumented aircraft (an Office of Naval Research Schweizer aircraft) in the vicinity of the 0°C isotherm often resulted in clogging of the instruments with graupel-type precipitation (C. B. Moore and H. J. Christian, private communication).
22. L. J. Battan, *Radar Observation of the Atmosphere* (Univ. of Chicago Press, Chicago, 1973).
23. M. A. Uman, C. E. Swanberg, J. A. Tiller, Y. T. Lin, *Radio Sci.* **11**, 985 (1976).
24. B. F. J. Schonland and H. Collens, *Proc. Roy. Soc. London Ser. A* **143**, 654 (1945).

B. F. J. Schonland, D. J. Malan, H. Collens, *ibid.* **152**, 595 (1935).

26. J. S. Boyle and R. E. Orville, *J. Geophys. Res.* **81**, 4461 (1976).
27. Technical Reports TR-25188 (1937), TR-25190 (1937), and TR-25192 (1939), General Electric Company, Pittsfield, Mass.
28. K. Berger, R. B. Anderson, H. Kroninger, *Elektra* **41**, 23 (1975).
29. W. W. Lewis and C. M. Foust, *Trans. Am. Inst. Electr. Eng.* **64**, 107 (1945).
30. S. Szpor, *IEEE Trans. Power Appar. Syst.* **PAS-88**, 646 (1969); F. Popolansky, *Elektra* **22**, 139 (1972).

31. We express appreciation to the National Aeronautics and Space Administration, especially the staff of Kennedy Space Center for coordinating and supporting the Thunderstorm Research International Program. The research reported here was funded in part by the following grants and contracts: University of Florida: ATM76-01454 (NSF), NGR-10-005-169 (NASA), and N00014-75-C-C-0143 (ONR); University of Arizona: NAS10-8518 (NASA) and N00014-76-C0206 (ONR); New Mexico Institute of Mining and Technology: ATM76-14917 (NSF) and N00014-76-C-0574 (ONR); and Rice University: DES 74-18765, DES 74-14456, and ATM76-17913 (NSF).

Neural Organization and Evolution of Thermal Regulation in Mammals

Several hierarchically arranged integrating systems may have evolved to achieve precise thermoregulation.

E. Satinoff

Much of the work in the field of temperature regulation has been devoted to elucidating the nature of the central thermostat. According to the generally accepted model of thermoregulation, the temperature of the body is detected by thermosensitive neurons which bring autonomic and behavioral mechanisms into play to counteract any deviations from the optimal state (see Fig. 1A). Inputs from the skin, brain, and body are summed in a comparator which also receives input from an intrinsic reference signal, the set point. The output of this comparator, or integrator (the two terms will be used interchangeably), is a single error signal which serves as an input to the controllers of the appropriate thermoregulatory responses, both autonomic and behavioral (*1*). The alteration in body temperature resulting from the performance of these responses is fed back to the comparator which, in turn, adjusts the error signal. Because the same signal activates all thermoregulatory responses the fact that some responses in an animal's thermal repertoire appear earlier

The author is a professor in the Departments of Psychology and Physiology and Biophysics, University of Illinois at Urbana-Champaign, Champaign 61820.